

Excitations in antiferromagnetic cores of superconducting vortices

Henrik Bruus, Kasper Astrup Eriksen, Michael Hallundbæk and Per Hedegård

*Ørsted Laboratory, Niels Bohr Institute for APG,
Universitetsparken 5, DK-2100 Copenhagen Ø Denmark*

(Submitted to Phys. Rev. B, July 10, 1998)

We study excitations of the predicted antiferromagnetically ordered vortex cores in the superconducting phase of the newly proposed $SO(5)$ model of strongly correlated electrons. Using experimental data from the literature we show that the susceptibilities in the spin sector and the charge sector are nearly equal, and likewise for the stiffnesses. In the case of strict equality $SO(5)$ symmetry is possible, and we find that if present the vortices give rise to an enhanced neutron scattering cross section near the so called π resonance at 41 meV. In the case of broken $SO(5)$ symmetry two effects are predicted. Bound excitations can exist in the vortex cores with “high” excitation energies slightly below 41 meV, and the massless Goldstone modes corresponding to the antiferromagnetic ordering of the core can acquire a mass and show up as core excitation with “low” excitation energies around 2 meV.

I. INTRODUCTION

Inspired by the discovery of a sharp antiferromagnetic resonance, later denoted the π resonance, in neutron scattering experiments on the superconducting phase of $YBa_2Cu_3O_7$ at (π, π) in the reciprocal space^{1,2} a new idea was introduced a year ago in the search for a theory of the high- T_c superconductors. Within the framework of the t - J limit of the Hubbard model^{3,4} it was shown theoretically already three years ago⁵ that the π resonance could be explained in terms of a new collective mode in the particle particle channel of the model, and that this mode is intimately connected with the symmetry of the superconducting gap. Pursuing the symmetry aspects of the problem Zhang proposed a theory combining antiferromagnetism and superconductivity by symmetry arguments.⁶ The operators responsible for the π resonance was identified with the six generators of rotation between the antiferromagnetic state and the superconducting state. Furthermore, it was proposed that the phase diagram of the cuprates can be understood as a competition at low temperatures between d -wave superconductivity and antiferromagnetism of a system which at higher temperatures posses $SO(5)$ symmetry. The group $SO(5)$ is sufficiently large to accommodate both the gauge group $U(1)$ ($= SO(2)$) which is broken in the superconducting state, and the spin rotation group $SO(3)$ which is broken in the antiferromagnetic state. In the simplest version the transition between the two ordered states is controlled by one parameter – the chemical potential for holes in the otherwise half-filled quadratic lattice of spin 1/2 fermions. The idea has generated a lot of discussion among theorists⁷⁻¹⁰, and no consensus on the matter has emerged.

We shall not enter this discussion here. Rather we will take the approach of assuming the model to be a fair description of the high- T_c materials and derive experimental consequences, which can be tested in the laboratory. Arovas *et al.*¹¹ have pointed out that in the

vortex cores of fluxoids in the superconducting state the order parameter will escape into the antiferromagnetic subspace, meaning that in these cores we have local antiferromagnetic moments instead of a simple featureless normal metal core. This unique prediction of the $SO(5)$ model should in principle be quite simple to verify experimentally. However, preliminary measurements¹² where one looked for Bragg-scattering from these moments belonging to the vortex cores did not produce any signal. This is perhaps not so surprising, since each of the vortex cores will form a one-dimensional magnet (along the c axis) and at finite temperatures such a system does not form long range order, and no Bragg peak is to be expected.

In this paper we are going to pursue the idea that in each copper-oxide plane small islands of antiferromagnetically ordered spins exist associated with the vortices generated by an external magnetic field. The direction of the spins in these islands will not be very strongly correlated from layer to layer and from island to island. In one island, however, there should exist excitations of the spins, a kind of bound spin wave modes or size quantized magnons. Using samples in the under-doped regime of the superconducting phase, where the proximity of the antiferromagnetic phase stabilizes the antiferromagnetic vortex cores¹¹, one should be able to pick up these core excitations in inelastic neutron scattering measurements. The modes can be classified according to the approximate symmetry: Two zero-energy or “low” energy Goldstone modes whose existence is guaranteed by the exact spin rotation symmetry, and two resonances or weakly bound “high” energy modes related to the π resonance arising from the approximate $SO(5)$ symmetry allowing for rotations between the d wave superconducting phase and the antiferromagnetic phase. Based on experimental data taken from the literature we discuss in Sec. II the $SO(5)$ model and its parameters. The values of the susceptibilities and the stiffnesses in the charge sector and the spin sector are found to be nearly equal, a remarkable

fact supporting the $SO(5)$ model. In Sec. III we set up the calculation for excitations of the vortex core. In the isotropic case we show analytically that the Goldstone modes of the vortex core indeed have zero energy, and that the vortex indeed generates a resonance reminiscent of the π resonance at the bottom of the continuum. In the anisotropic case the Goldstone modes remains massless, but for certain anisotropies the π resonance can be transformed into a bound state localized at the vortex. Treating the external fields more accurately introduces symmetry-breaking terms in the Hamiltonian and results in finite masses to the Goldstone modes. This will be discussed in Sec. IV. Concluding remarks are contained in Sec. V.

II. THE $SO(5)$ MODEL AND ITS PARAMETERS

In the $SO(5)$ model the relevant order parameter is a real vector \mathbf{n} in a five dimensional superspin space with a length which is fixed at low temperatures,

$$\mathbf{n} = \{n_1, n_2, n_3, n_4, n_5\}, \quad |\mathbf{n}|^2 = 1. \quad (1)$$

This order parameter is related to the complex superconductor order parameter, ψ , and the antiferromagnetic order parameter, \mathbf{m} , in each copper-oxide plane as follows:

$$\psi = f e^{i\theta} = n_1 + i n_5, \quad \mathbf{m} = (n_2, n_3, n_4). \quad (2)$$

In Ref. 6 Zhang argued how in terms of the five dimensional superspin space one can construct an effective Lagrangian $\mathcal{L}(\mathbf{n})$ describing the low energy physics of the t - J model. In the absence of external electromagnetic fields it takes the form

$$\begin{aligned} \mathcal{L}(\mathbf{n}) = & \sum_{a < b} \frac{\chi_{ab}}{2} \left[n_a \left(\partial_t n_b - \frac{2\mu}{\hbar} \{ \delta_{b,1} n_5 - \delta_{b,5} n_1 \} \right) - (a \leftrightarrow b) \right]^2 \\ & - \sum_{a < b} \frac{\rho_{ab}}{2} \left[n_a \nabla n_b - n_b \nabla n_a \right]^2 + \frac{1}{2} g (n_2^2 + n_3^2 + n_4^2), \quad (3) \end{aligned}$$

where the indices run from 1 through 5.

The generalized susceptibilities, χ , fall in three groups: $\chi_c \equiv \chi_{15}$ connecting the charge sector $\{n_1, n_5\}$ with itself, $\chi_s \equiv \chi_{23} = \chi_{24} = \chi_{34}$ connecting the spin sector $\{n_2, n_3, n_4\}$ with itself, and $\chi_\pi \equiv \chi_{1(2,3,4)} = \chi_{(2,3,4)5}$ connecting the spin sector with the charge sector. Similarly with the stiffnesses: $\rho_c \equiv \rho_{15}$, $\rho_s \equiv \rho_{23} = \rho_{24} = \rho_{34}$, and $\rho_\pi \equiv \rho_{1(2,3,4)} = \rho_{(2,3,4)5}$. Below, based on experimental data, we find that $\rho_s \approx \rho_c$ and $\chi_s \approx \chi_c$. It is a remarkable fact that the dynamics in two such distinct sectors as the charge and the spin sector are governed by coupling strengths of the same size, and it can be taken as one strong indication of the near $SO(5)$ symmetry of the cuprates. At present the values of χ_π and ρ_π are not

known experimentally, and it is part of our work to establish a method to measure them. If the corresponding coupling strengths are the same in all sectors we denote it the isotropic case, otherwise the anisotropic case.

In the following we estimate on a 25 % accuracy level the typical zero temperature values of the parameters of the $SO(5)$ model obtained for various cuprates of the form $YBa_2Cu_3O_{6+x}$ (YBCO) and $La_{2-x}Sr_xCuO_4$ (LSCO) with a range of doping levels x . All numerical values are listed in Table I. First we note that for both materials the Cu-O-Cu distance¹³ is $a = 3.8 \text{ \AA}$. However, YBCO contains two CuO planes over a distance of 11.4 \AA (the sum of the alternating inter-layer distances 3.2 \AA and 8.2 \AA), while LSCO contains one CuO plane every 6.6 \AA . Hence, when needed for normalization purposes we employ $c = 6.1 \text{ \AA}$ as the typical inter-layer distance.

From the upper critical field H_{c2} the typical correlation length is found to be $\xi \simeq 16 \text{ \AA}$,¹⁴ while many different methods like muon spin rotation, magnetic torque, magnetization, and kinetic inductance (see Ref. 15 and references therein) all result in a London length, $\lambda_L \simeq 1350 \text{ \AA}$. Thus the Ginzburg-Landau parameter is $\kappa = \lambda_L/\xi \simeq 84$.

The connection between the generalized coefficients and the directly measurable parameters are given below. In the completely isotropic case where all generalized coefficients are equal we have:¹¹

$$\tilde{g} = g - \chi(2\mu/\hbar)^2, \quad (4)$$

$$\xi = \sqrt{\rho/(-\tilde{g})}, \quad (5)$$

$$\lambda_L = \frac{\hbar}{2e} \sqrt{c/\rho\mu_0}. \quad (6)$$

To estimate ρ_s and χ_s of the spin sector, experimental measurements are combined with theoretical calculations of spin waves within the two dimensional spin 1/2 quantum Heisenberg model of antiferromagnetism.¹⁶⁻¹⁸ The bare coupling constant J is related to ρ_s , χ_s and the spin wave velocity v_s as¹⁸

$$\rho_s = Z_\rho J/4 \quad (7)$$

$$\chi_s = Z_\chi p_a^2/8J \quad (8)$$

$$v_s = Z_c \sqrt{\rho/\chi} = Z_c \sqrt{2J/p_a}, \quad (9)$$

$$Z_\rho = 0.72, \quad Z_\chi = 0.51, \quad Z_c = 1.18, \quad (10)$$

where for brevity a momentum $p_a \equiv \hbar/a$ has been introduced, and where the Z 's are renormalization constants, which for classical spin waves all equals 1, but differs from 1 when quantum fluctuations and spin wave interactions are taken into account. Neutron scattering experiments on LSCO¹⁹ have led to a determination of v_s and from that to $J = 132 \text{ meV}$ in agreement with other experiments. From J one calculates $\rho_s = 24 \text{ meV}$. Independently, ρ_s have been determined by neutron scattering measurement²⁰ of the antiferromagnetic correlation length $\xi_{AFM}(T) \propto \exp(2\pi\rho_s/k_B T)$ also leading to $\rho_s = 24 \text{ meV}$. From Eq. (8) one finds

$a = 3.8 \text{ \AA}$	$\pi\xi^2/a^2 \simeq 56$	$c = 6.1 \text{ \AA}$
$\xi \simeq 16 \text{ \AA}$	$\lambda_L \simeq 1350 \text{ \AA}$	$\kappa \simeq 84$
$J \simeq 0.130 \text{ eV}$	$g \simeq 9 \text{ meV/\AA}^2$	$\tilde{g} \simeq -53 \text{ \mu eV/\AA}^2$
$\rho_s \simeq 0.024 \text{ eV}$	$\chi_s/p_a^2 \simeq 0.49 \text{ eV}^{-1}$	$\delta_\rho > -1$
$\rho_c \simeq 0.018 \text{ eV}$	$\chi_c/p_a^2 \simeq 0.42 \text{ eV}^{-1}$	$\delta_\chi > -0.014$

TABLE I. The average values of typical parameters of the $SO(5)$ model based on experimental data for YBCO and LSCO as described in the text. The Cu-O-Cu distance is denoted a , while the average distance between the CuO planes is denoted c . For brevity a momentum $p_a \equiv \hbar/a$ has been introduced. The number of spins in a given vortex core is estimated by $\pi\xi^2/a^2$. The anisotropy parameters δ_ρ and δ_χ are defined in Sec. IIIB.

$\chi_s/p_a^2 = 0.49 \text{ eV}^{-1}$. A more recent neutron scattering experiment on LSCO²¹ yielded the consistent result $Z_\chi = 0.4 \pm 0.1$ and $J = 125 \text{ meV}$.

In the charge sector we have $\rho_c = (c/\mu_0)(\hbar/2e\lambda_L)^2$, while $\chi_c = \rho_c/v_c^2$, where v_c is the sound velocity of the electron liquid. The charge stiffness is readily obtained from the London length, $\rho_c = (\hbar/2e)^2(c/\mu_0)(1/\lambda_L)^2 \approx 18 \text{ meV}$. The susceptibility χ_c is obtained as follows. In ordinary superconductors the Goldstone mode corresponding to the sound velocity is rendered massive by the Anderson-Higgs mechanism and turned into a plasmon mode²², but as a theoretical concept it can be calculated, and it is found to be of the order of the Fermi velocity, v_F . Detailed studies^{13,23} have shown that the dispersion relation for quasi particles moving around on the lattice of the t - J model at low doping near half filling is governed not by t but is renormalized $t^* \approx J$. Using the dispersion relation (3.15) of Ref. 13, $\varepsilon_{\mathbf{k}} = \text{const} + J \cos(k_x a) \cos(k_y a) + \frac{1}{3}J[\cos(2k_x a) + \cos(2k_y a)]$, yields $v_c \approx v_F \approx 1.58J/p_a$. From this we find $\chi_c/p_a^2 \approx 0.42 \text{ eV}^{-1}$.

To estimate the value of the phenomenological symmetry breaking constant g in Eq. (3) we consider complete antiferromagnetic ordering, *i.e.* $|\mathbf{m}|^2 = 1$. In this case the ordering energy density in the $SO(5)$ model is simply $-\frac{1}{2}g|\mathbf{m}|^2 = -\frac{1}{2}g$. On the other hand this energy density can also be expressed within the t - J model as $-J/(2a^2)$, and therefore $g = J/a^2 \simeq 9 \text{ meV \AA}^{-2}$. The effective coupling constant \tilde{g} of Eq. (4) is much smaller. Anticipating the discussion in Sec. III A of the π resonance frequency $\omega_\pi \approx 41 \text{ meV}$ we find the following estimate: $\tilde{g} = -\chi_\pi \omega_\pi^2 \simeq -53 \text{ \mu eV/\AA}^2$.

III. VORTICES AND CORE EXCITATIONS IN THE $SO(5)$ MODEL

In Ref. 11 the vortex solutions to the isotropic $SO(5)$ model have been studied in great detail. To study the anisotropic case we are going to use a different method. To establish our method and notation, we will start out in Sec III A by deriving some of the known results for the

isotropic case, before in Sec IIIB we continue with the anisotropic case.

A. Vortices and resonances in the isotropic case

In the symmetric version of the $SO(5)$ model the generalized susceptibilities and stiffnesses are isotropic in spin space, and the only symmetry breaking terms are quadratic terms governed by the chemical potential μ and the phenomenological constant g chosen such that superconductivity is favored. The external electromagnetic fields will now be included through the vector potential \mathbf{A} . However, in this section we only keep the interaction with the ψ part of the order parameter this being the dominating part of the external fields. In Sec. IV A we will include the Zeeman interaction between \mathbf{A} and the \mathbf{m} part of the order parameter and demonstrate explicitly that this only leads to minor changes. In this approximation the Lagrangian \mathcal{L}_{iso} then has the form:

$$\begin{aligned} \mathcal{L}_{\text{iso}} = & \frac{1}{2}\chi|\partial_t\psi|^2 + \frac{1}{2}\chi|\partial_t\mathbf{m}|^2 + \\ & -\frac{1}{2}\rho\left|\left(\nabla + \frac{i2e}{\hbar}\mathbf{A}\right)\psi\right|^2 - \frac{1}{2}\rho|\nabla\mathbf{m}|^2 \\ & -\frac{1}{2}\chi\left(\frac{2\mu}{\hbar}\right)^2|\psi|^2 + \frac{1}{2}g\mathbf{m}^2 + \frac{1}{2}\lambda(1-|\psi|^2-\mathbf{m}^2) \\ & + \frac{c}{2\mu_0}\left(\frac{1}{c_0^2}|\partial_t\mathbf{A}|^2 - |\nabla\times\mathbf{A}|^2\right), \end{aligned} \quad (11)$$

where c is the lattice constant perpendicular to the copper-oxide planes and c_0 the speed of light. For later convenience we have incorporated the constraint Eq. (1) through the Lagrange multiplier λ . Using dimensionless polar coordinates (s, ϕ) , with $s \equiv r/\xi$, centred at the origin of the vortex core, we seek solutions of the form

$$\psi(s, \phi) = f(s)e^{-i\phi}, \quad \mathbf{m} = m(s)\mathbf{e}_\beta, \quad \mathbf{A} = \frac{\hbar}{2e\xi} \frac{\alpha(s)}{s} \mathbf{e}_\phi, \quad (12)$$

where \mathbf{e}_β is an arbitrary unit vector in (n_2, n_3, n_4) -space (equivalent to real space) taken to be $(0, 1, 0)$ in the following, while \mathbf{e}_ϕ is the azimuthal unit vector. The Euler-Lagrange equation for λ yields the constraint

$$f(s)^2 + \mathbf{m}(s)^2 = 1, \quad (13)$$

such that once $f(s)$ is determined so is $m(s)$. The Euler-Lagrange equation for \mathbf{m} is used to express $\lambda(s)$ in terms of $m(s)$:

$$\frac{1}{m}\nabla^2 m = \frac{(\lambda - g)\xi^2}{\rho}. \quad (14)$$

Eqs. (13) and (14) are then used to eliminate $m(s)$ and $\lambda(s)$ in the Euler-Lagrange equation for $f(s)$, and as in Ref. 11 we end up with:

$$\nabla^2 f + \frac{f}{1-f^2} (\partial_s f)^2 + f(1-f^2) \left[1 - \left(\frac{\alpha-1}{s} \right)^2 \right] = 0. \quad (15)$$

The Euler-Lagrange equation for $\alpha(s)$ becomes

$$\partial_s^2 \alpha - \frac{1}{s} \partial_s \alpha = \frac{(\alpha-1)}{\kappa^2} f^2. \quad (16)$$

Equations (15) and (16) are solved by the numerical shooting method¹¹ and yields $f(s)$ and $\alpha(s)$.

Introducing the “effective potential” $V_0(s)$ as the right hand side of equation Eq. (14),

$$V_0(s) \equiv \frac{(\lambda-g)\xi^2}{\rho} = \frac{1}{m} \nabla^2 m = -\frac{f \nabla^2 f}{(1-f^2)} - \frac{(\partial_s f)^2}{(1-f^2)^2}, \quad (17)$$

we can use the solution of $f(s)$ to determine $V_0(s)$, which in turn results in the Euler-Lagrange equation for \mathbf{m} of the form

$$[-\nabla^2 + V_0(s)] m = 0. \quad (18)$$

Naturally, by construction, Eq. (18), is automatically fulfilled using $m(s) = \sqrt{1-f(s)^2}$, but for the forthcoming studies of core excitations it is useful to think of the static core as corresponding to the zero energy solution of the Schrödinger-like equation Eq. (18) where $V_0(s)$ clearly plays the role of an effective potential. For the same reasons we rewrite Eq. (15) for $f(s)$ by the use of Eq. (17) for $V_0(s)$:

$$\left[-\nabla^2 + \frac{1}{s^2} + V_0(s) + \frac{\alpha(2-\alpha)}{s^2} \right] f = f. \quad (19)$$

Thus having established the notation and found the static vortex solutions we now turn to the problem of finding excitations in the vortex core. We denote the static vortex solution by \mathbf{n}_0 , and due to the $SO(3)$ symmetry in the spin sector we are free to choose the direction of \mathbf{n}_0 at will. In anticipation of the treatment in Sec. IV A where an external magnetic field in the z direction forces \mathbf{n}_0 to lie in the xy plane we choose $\mathbf{n}_0 \propto \mathbf{e}_y$, *i.e.* only the second of the three \mathbf{n}_0 components is nonzero:

$$\mathbf{n}_0 = \{f(s) \cos(\phi), 0, m(s), 0, -f(s) \sin(\phi)\}. \quad (20)$$

We seek excitations $\delta \mathbf{n}$ which are of lowest order in the deviations $\delta \psi$ and $\delta \mathbf{m}$. These turns out to be perpendicular to \mathbf{n}_0 , *i.e.* $\delta \mathbf{n} \propto \mathbf{e}_x$ or $\delta \mathbf{n} \propto \mathbf{e}_z$ or linear combinations thereof, and hence of the form

$$\begin{aligned} \delta \mathbf{n}_x &= \{0, 1, 0, 0, 0\} \delta m, \\ \delta \mathbf{n}_z &= \{0, 0, 0, 1, 0\} \delta m, \\ \delta m &= \delta m_{nl}(s) e^{il\phi} e^{-i\omega t}. \end{aligned} \quad (21)$$

Throughout this work we are dealing with cylindrical symmetric vortices, so the excitations are characterized

by the angular momentum l and the radial index n . Of course, $\delta \mathbf{n}$ is not a complex vector, so the notation $\exp(il\phi)$ is merely a short hand notation for either $\cos(l\phi)$ or $\sin(l\phi)$. The Lagrangian is now written to second order in $\delta \mathbf{n}$ as $\mathcal{L} = \mathcal{L}_{\text{iso}}^{(0)}(\mathbf{n}_0) + \mathcal{L}^{(2)}(\delta \mathbf{n})$. The explicit form of the second order term is

$$\mathcal{L}^{(2)}(\delta \mathbf{n}) = \frac{1}{2} \chi |\partial_t \delta \mathbf{n}|^2 - \frac{1}{2} \rho |\nabla \delta \mathbf{n}|^2 + \frac{1}{2} [g - \lambda(s)] |\delta \mathbf{n}|^2. \quad (22)$$

Assuming solutions $\delta \mathbf{n}$ of the form given in Eq. (21) the Euler-Lagrange equation for $\delta m_{nl}(s)$ then takes the form of the following eigenvalue equation:

$$\begin{aligned} \left[-\nabla^2 + \frac{l^2}{s^2} + V_0(s) \right] \delta m_{nl} &= \varepsilon \delta m_{nl}, \\ \varepsilon &= \frac{\chi \xi^2}{\rho} \omega^2 = \frac{\chi}{-\tilde{g}} \omega^2. \end{aligned} \quad (23)$$

Using the approximate $SO(5)$ symmetry we can immediately find two analytical solutions δm_{00} and δm_{01} to Eq. (23). Due to the exact spin rotation symmetry it does not cost any energy to rotate the order parameter \mathbf{n}_0 of Eq. (20) in spin space. Rotating \mathbf{n}_0 a small angle $\delta\theta$ in the (n_3, n_4) plane produces the deviation $\delta \mathbf{n}_{00} = \{0, 0, 0, \delta\theta m(s), 0\}$. If the trial solution $\delta m_{00}(s) \propto m(s)$ is used (note that $l = 0$), we see from Eq. (18) that as expected Eq. (23) is satisfied with $\varepsilon = 0$. Thus in the the effective potential description the ground state vortex configuration corresponds to a zero energy and zero angular momentum mode.

The second solution is found by rotating between the charge sector and the spin sector. In a perfect $SO(5)$ symmetric model such a rotation does not cost any energy. However, one central idea in the $SO(5)$ model of high T_c superconductors is that the $SO(5)$ symmetry is only approximate. It costs a finite energy to rotate between the spin and charge sectors. Experimentally this is reflected by the 41 meV π resonance, and theoretically by the symmetry breaking term $\frac{1}{2} g \mathbf{m}^2$ of Eq. (3). We thus expect that by rotating \mathbf{n}_0 a small angle $\delta\theta$ in the (n_1, n_4) plane a deviation $\delta \mathbf{n}_{01} = \{0, 0, 0, \delta\theta f(s) \cos(\phi), 0\}$ is produced which is an eigen-excitation with $\varepsilon > 0$. If the trial solution $\delta m_{01}(s) \propto f(s) \cos(\phi)$ is inserted into Eq. (23) (note that $l = 1$), we obtain

$$\left[-\nabla^2 + \frac{1}{s^2} + V_0(s) \right] f = \varepsilon f. \quad (24)$$

It is seen from Eq. (19) that this equation is indeed satisfied by $f(s)$ if $\varepsilon = 1$ and if the additional potential $\alpha(2-\alpha)/s^2$ can be neglected. It turns out that the large value of the Ginzburg-Landau parameter, $\kappa \simeq 84$, indeed does make the additional potential negligible. Numerical calculations show $\alpha(2-\alpha)/s^2 < 0.001$ (for any value of s) which is much smaller than $V_0(s) \simeq 1$ and $\varepsilon = 1$. The approximate nature of the solution is not surprising,

since the external magnetic field does in fact break the $SO(5)$ symmetry by coupling only to the (n_1, n_5) components of the order parameter. However, the larger a value of κ the weaker this symmetry breaking appears, and in the limit of infinite κ the approximate solution becomes exact. Since the ground state energy is set to be zero as the zero energy mode, the excitation energy of the δm_{01} resonance is given by $\varepsilon = 1$, or going back to frequency: $\omega_\pi = \sqrt{-\tilde{g}/\chi}$, which is in accordance with that of the π resonance given in Ref. 6.

In conclusion we note that both δm_{00} and δm_{01} contains no radial nodes, hence the notation $n = 0$. Any other excitation or resonance would contain more nodes and thus have higher energies. Since δm_{01} corresponds to a resonance at the bottom edge of the continuum we can infer that for the isotropic case no bound collective excitations exist in the antiferromagnetic vortex core.

B. Vortices and excitations in the anisotropic case

We now turn to the anisotropic case. As discussed in Sec. II $\rho_s \approx \rho_c$ and $\chi_s \approx \chi_c$. In the following we therefore study the consequences of anisotropies arising from $\rho_\pi \neq \rho_s = \rho_c$ and $\chi_\pi \neq \chi_s = \chi_c$:

$$\begin{aligned} \rho &\equiv \rho_s = \rho_c, & \chi &\equiv \chi_s = \chi_c, \\ \rho_\pi &\equiv \rho + \Delta\rho, & \chi_\pi &\equiv \chi + \Delta\chi, \\ \delta_\rho &\equiv \Delta\rho/\rho, & \delta_\chi &\equiv \Delta\chi/\chi. \end{aligned} \quad (25)$$

These anisotropies are not known experimentally, and it is part of our work to establish a method to measure it. We begin by finding constraints on them. The stiffness has to be a positive number, *i.e.* $\rho_\pi = \rho(1 + \delta_\rho) > 0$ or $\delta_\rho > -1$. The π susceptibility χ_π is related to the π resonance and to the coupling strengths g and \tilde{g} . Defining $\gamma \equiv (g - \tilde{g}_0)/g$, where the subscript 0 refer to the isotropic case, we can estimate γ using the values listed in Table I and find $\gamma \simeq 1.014$. The relation between \tilde{g} and \tilde{g}_0 can be written as

$$\tilde{g} = g - \chi_\pi \left(\frac{2\mu}{\hbar}\right)^2 = \tilde{g}_0 \frac{1 - (1 + \delta_\chi)\gamma}{1 - \gamma}. \quad (26)$$

To ensure the superconducting phase it is mandatory to have $\tilde{g} < 0$ and hence from the enumerator in Eq. (26) that $1 - (1 + \delta_\chi)\gamma < 0$ or $-0.014 < \delta_\chi$. This constraint is listed in Table I.

The Lagrangian $\mathcal{L}_{\text{ani}} = \mathcal{L}_{\text{iso}} + \Delta\mathcal{L}$ in the anisotropic case differs from the Lagrangian \mathcal{L}_{iso} in the isotropic case by $\Delta\mathcal{L}$ containing terms proportional to the anisotropies δ_ρ and δ_χ . The Euler-Lagrange equations for f , m , and α corresponding to \mathcal{L}_{ani} become

$$\begin{aligned} \nabla^2 f + \frac{f(\partial_s f)^2}{1 - f^2} + \left[1 - \left(\frac{\alpha - 1}{s}\right)^2\right] f(1 - f^2) \\ = \left[\frac{2\delta_\chi}{1 + \delta_\chi} \left(1 - \frac{g}{\tilde{g}}\right) - \frac{2\delta_\rho}{1 + \delta_\rho} \left(\frac{\alpha - 1}{s}\right)^2\right] f^3(1 - f^2), \end{aligned} \quad (27)$$

$$\frac{\nabla^2 m}{m} = \frac{(\lambda - g)\xi^2}{\rho_\pi} + \frac{\delta_\rho}{1 + \delta_\rho} [(\nabla m)^2 + m\nabla^2 m], \quad (28)$$

$$\partial_s^2 \alpha = \frac{1}{s} \partial_s \alpha + \frac{\alpha - 1}{\kappa^2} f^2 \left[1 - \frac{\delta_\rho}{1 + \delta_\rho} f^2\right]. \quad (29)$$

It is seen how the anisotropy leads to more nonlinear terms in the differential equations. Using the same numerical methods as in Sec. III A we study the static vortex cores for various values of δ_ρ and δ_χ . Some results are shown in Fig. 1.

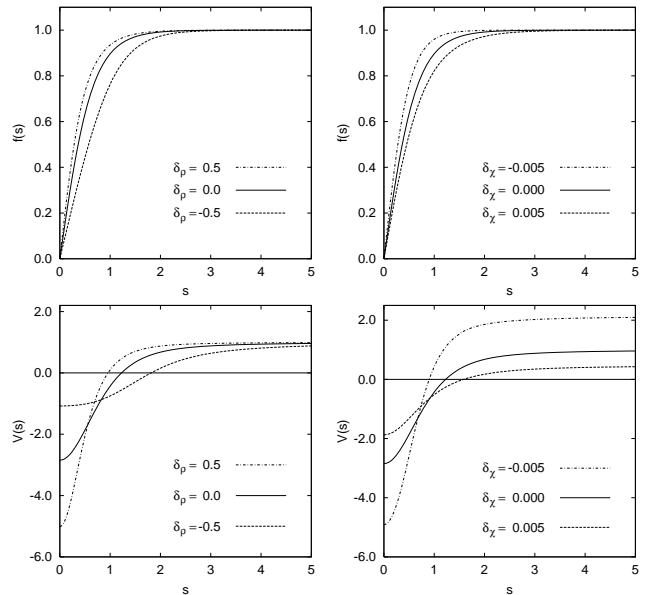


FIG. 1. A display of the vortex cores for various values of the anisotropy parameters. Graphs of the modulus $f(s)$ of the superconducting order parameter as well as of the effective potential $V(s)$. The parameters are $\kappa = 84$ and $\gamma = 1.014$. When δ_ρ is varied, $\delta_\chi = 0$ and vice versa.

In the isotropic case the static vortex core led to an effective potential description with $V_0(s)$ defined as the right hand side of Eq. (14). Similarly, for the anisotropic case we now define an effective potential $V(s)$ as the right hand side of Eq. (28) which then satisfies the equation

$$[-\nabla^2 + V(s)] m = 0. \quad (30)$$

$V(s)$ can be expressed in terms of f by using $m^2 = 1 - f^2$, and thus it can be found by solving Eqs. (28) and (29). Due to the anisotropy the effective potential and hence the excitation spectrum changes. The effective potential for some anisotropy parameters are shown in Fig. 1. We study the transverse excitations given by Eq. (21) and find the following eigenvalue equation to be fulfilled by $\delta m_{nl}(s)$:

$$[-\nabla^2 + \frac{l^2}{s^2} + V(s)] \delta m_{nl} = \frac{\xi^2 \chi_\pi}{\rho_\pi} \omega^2 \delta m_{nl} = \varepsilon \delta m_{nl}. \quad (31)$$

As in the isotropic case a zero energy solution corresponding to the static vortex solution is trivially given.

What is new in the anisotropic case is that now bound excitations do exist with $\varepsilon < V(\infty)$. Some of them are shown in Fig. 2.

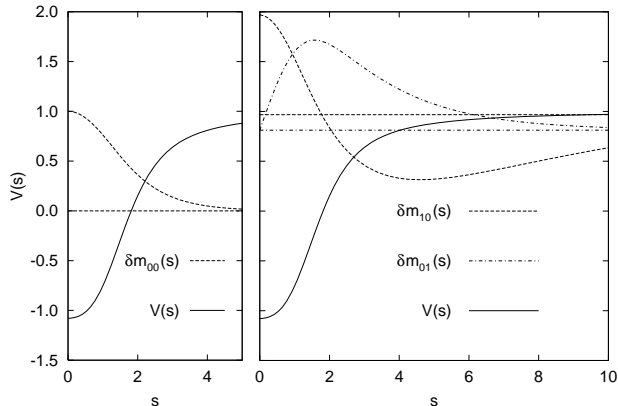


FIG. 2. The radial part δm_{nl} of bound antiferromagnetic excitations in the vortex core in an anisotropic case. To show the effects more clearly we have chosen the rather extreme parameter value $\delta_\rho = -0.5$, while having $\kappa = 84$, $\delta_\chi = 0$, and $\gamma = 1.014$. To the left is shown the zero energy state δm_{00} corresponding to the static vortex core. To the right are shown the first two excitations δm_{01} and δm_{10} above the zero energy mode. The full line in both panels is the effective potential $V(s)$. The ordinate axis accounts for $V(s)$ in the energy units of Eq. (31). The excitations δm_{nl} are given in arbitrary units. The eigenenergies are represented by the dashed horizontal lines with $\varepsilon_{00} = 0.00$, $\varepsilon_{01} = 0.81$, and $\varepsilon_{10} = 0.97$.

In Fig. 3 we plot as a function of the anisotropy parameter δ_ρ the energy of the lowest excited state δm_{01} above the ever present zero energy mode δm_{00} . It is seen how δm_{01} evolves from the scattering resonance, the π resonance, discussed in Sec. III A with $\varepsilon = V(\infty)$ at the isotropic point $\delta_\rho = 0$ to a strongly bound state with $\varepsilon = 0$ at $\delta_\rho = -1$, the largest negative value allowed. At this point the excited state thus coincide energetically with the zero energy state indicating the phase transition from superconductivity to antiferromagnetism – the gap of the π excitations has collapsed.

Our calculations thus lead to the following prediction. For a given anisotropy $\delta_\rho < 0$ neutron scattering will in zero magnetic field show the π resonance with $\varepsilon = V_{\text{ani}}(\infty)$ or frequency $\omega = \omega_\pi$. As the magnetic field is turned on more and more vortices are created. Each of them supports a δm_{01} excitation with an energy $\varepsilon_{01} < V(\infty)$ or frequency $\omega_{01} < \omega_\pi$. Consequently an excitation resonance should show up at the low-energy side of the π resonance, and the amplitude of this resonance scales with the magnetic field.

Similar results does not hold for $\delta_\chi \neq 0$. The reason for this can be traced back to the behavior of V shown in Fig. 1. When δ_χ is made positive the potential widens as in the case of negative δ_ρ , however, at the same time the asymptotic value drops. As a result no excitations are bound in the potential. In the case of negative δ_χ the po-

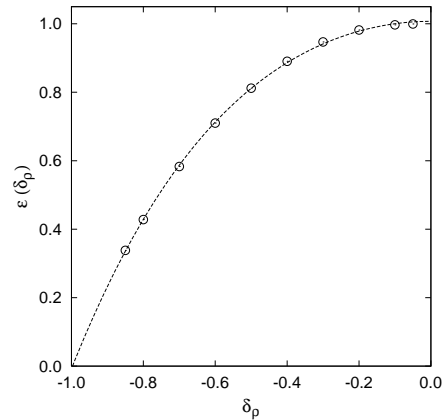


FIG. 3. The energy ε of the lowest bound excitation as a function of the anisotropy δ_ρ for $\kappa = 84$, $\delta_\chi = 0$, and $\gamma = 1.014$. The dotted line is a fit, $\varepsilon(\delta_\rho) \simeq 1.0 - 0.7\delta_\rho^2 - 0.3\delta_\rho^4$. Note that $\varepsilon(0) = 1$ and $\varepsilon(-1) = 0$.

tential narrows down, but although the asymptotic value rises, it does not rise enough to bind any excitations.

It should be added that this change in the asymptotic value of V due to δ_χ is in accordance with the result for the π resonance in a bulk superconductor without the presence of vortices. In the dimensionless units of the problem, see Eq. (23), the frequency ω_π of the π resonance is given by

$$\frac{\chi_\pi \omega_\pi^2}{-\tilde{g}} = 1 + 2 \frac{\Delta\chi (2\mu)^2}{\tilde{g} \hbar^2} = \frac{(1-\gamma) + \delta_\chi \gamma}{(1-\gamma) - \delta_\chi \gamma}. \quad (32)$$

Inserting the values $\delta_\chi = -0.005$, 0 , and 0.005 we find 2.14, 1.00, and 0.47, respectively, as $V(\infty)$ in Fig. 1.

IV. GOLDSTONE MODES

In Sec. III we studied the zero energy modes and the excitations of the antiferromagnetic order parameter \mathbf{m} in the superconducting vortex core. The zero energy modes $\delta \mathbf{n}_x$ and $\delta \mathbf{n}_z$ in Eq. (21) were found to be degenerate gapless Goldstone modes. This degeneracy is a result of two approximations, one being the neglect of the Zeeman interaction between \mathbf{m} and the external magnetic field \mathbf{B} , the other being the neglect of inter-layer interaction between the spins. In this section we show how the degeneracies are lifted and massive Goldstone modes appear when the approximations are abandoned.

A. Coupling of core excitations to the external magnetic field

The primary effect of the external magnetic field $\mathbf{B} = B\mathbf{e}_z$ on the system is the creation of superconducting vortices through the interaction with the superconducting order parameter ψ . To a good approximation the

antiferromagnetic core described by \mathbf{m} can be treated disregarding the Zeeman coupling between \mathbf{B} and \mathbf{m} . We now take this coupling into account. Using standard field theoretic methods²⁴ the spin operator $\hat{\mathbf{S}}_j$ acting on site j can be expressed by a classical field \mathbf{h}_j ,

$$\hat{\mathbf{S}}_j \longrightarrow s e^{i\mathbf{Q}\cdot\mathbf{R}_j} \mathbf{h}_j, \quad (33)$$

where $s = 1/2$ and $\mathbf{Q} = \pi(a^{-1}, a^{-1}, c^{-1})$ is the antiferromagnetic ordering vector. We then have $\exp[i\mathbf{Q}\cdot\mathbf{R}_j] = (-1)^j$, *i.e.* 1 on sublattice A and -1 on sublattice B. Since the system is close to be completely antiferromagnetically ordered \mathbf{h}_j is written as

$$\mathbf{h}_j = \mathbf{m}_j + (-1)^j \mathbf{l}_j, \quad (34)$$

where \mathbf{l}_j denotes a small ferromagnetic component on top of the antiferromagnetic background \mathbf{m}_j . Both \mathbf{l}_j and \mathbf{m}_j are slowly varying fields in space. The rapid antiferromagnetic variation from site to site is explicitly taken into account by prefactors $(-1)^j$. The smallest deviation possible is obtained by having \mathbf{l}_j perpendicular to \mathbf{m}_j , and since \mathbf{h}_j is normalized to unity, we obtain to lowest order in \mathbf{l}_j that

$$|\mathbf{h}_j|^2 = 1, \quad \mathbf{l}_j \cdot \mathbf{m}_j = 0, \quad |\mathbf{m}_j|^2 = 1. \quad (35)$$

The Hamiltonian \hat{H}_B corresponding to the coupling between the spins and \mathbf{B} is

$$\hat{H}_B = \sum_j g^* \mu_B \hat{\mathbf{S}}_j \cdot \mathbf{B} \longrightarrow \frac{1}{2} g^* \mu_B \mathbf{B} \cdot \sum_j (-1)^j \mathbf{h}_j. \quad (36)$$

Only the ferromagnetic component yields a non-zero contribution to the sum, and after taking the continuum limit we end with a Lagrangian density \mathcal{L}_B given by

$$\mathcal{L}_B = -\frac{1}{2} \frac{g^* \mu_B}{a^2} \mathbf{B} \cdot \mathbf{l}(\mathbf{r}). \quad (37)$$

The appearance of a non-zero ferromagnetic component $\mathbf{l}(\mathbf{r})$ leads to a loss of antiferromagnetic ordering energy. This has to be included in the description through the Hamiltonian \hat{H}_{AFM} describing the spin-spin interaction:

$$\hat{H}_{\text{AFM}} = J \sum_{\langle j, j' \rangle} \hat{\mathbf{S}}_j \cdot \hat{\mathbf{S}}_{j'} \longrightarrow -\frac{1}{4} J \sum_{\langle j, j' \rangle} \mathbf{h}_j \cdot \mathbf{h}_{j'}. \quad (38)$$

Performing the sum and taking the continuum limit results in the Lagrangian density \mathcal{L}_{AFM} ,

$$\mathcal{L}_{\text{AFM}} = \frac{1}{2} \frac{J}{a^2} [1 - \mathbf{l}(\mathbf{r})^2]. \quad (39)$$

The constraint $\mathbf{l}_j \cdot \mathbf{m}_j = 0$ is incorporated through a Lagrange multiplier λ' and we end with the following Lagrangian density \mathcal{L}' of the magnetic effects

$$\mathcal{L}' = -\frac{1}{2} \frac{J}{a^2} \mathbf{l}(\mathbf{r})^2 + \left(\lambda' \mathbf{m} - \frac{1}{2} \frac{g^* \mu_B}{a^2} \mathbf{B} \right) \cdot \mathbf{l}(\mathbf{r}) + \frac{1}{2} \frac{J}{a^2}. \quad (40)$$

An effective Lagrangian $\mathcal{L}_{\text{mB}}(\mathbf{m})$ for the interaction between \mathbf{m} and \mathbf{B} is found from the partition function $Z = \int \mathcal{D}\mathbf{m} \int \mathcal{D}\mathbf{l} \int \mathcal{D}\lambda' \exp[iS(\mathbf{m}, \mathbf{l}, \lambda')/\hbar] = \int \mathcal{D}\mathbf{m} \exp[iS_{\text{eff}}(\mathbf{m})/\hbar]$ from which the final result can be extracted after integrating out \mathbf{l} and λ' :

$$\mathcal{L}_{\text{mB}}(\mathbf{m}) = -\frac{1}{2} \Gamma (\mathbf{B} \cdot \mathbf{m})^2 + \frac{1}{2} \Gamma \mathbf{B}^2 + \frac{1}{2} \frac{J}{a^2}, \quad (41)$$

where $\Gamma = (g^* \mu_B)^2 / (4Ja^2)$. Adding \mathcal{L}_{mB} to the Lagrangian of the anisotropic case \mathcal{L}_{ani} leads to the following eigenvalue equation for an excitation $\delta \mathbf{n}_\beta = \delta m \mathbf{e}_\beta$, with $\beta = x$ or z ,

$$[-\nabla^2 + V(s)] \delta m = \frac{\xi_\pi^2 \chi_\pi}{\rho_\pi} \left[\omega^2 - \frac{\Gamma}{\chi_\pi} B^2 \mathbf{e}_z \cdot \mathbf{e}_\beta \right] \delta m. \quad (42)$$

As was the case for Eq. (23) two eigensolutions proportional to m can now be found. One mode has $\beta = x$ (*i.e.* $\mathbf{e}_z \cdot \mathbf{e}_\beta = 0$) and remain a zero energy mode:

$$\hbar \omega_x = 0. \quad (43)$$

The other mode has $\beta = z$ (*i.e.* $\mathbf{e}_z \cdot \mathbf{e}_\beta = 1$), resulting in a nonzero energy, which can be estimated by setting $B = \Phi_0 / \pi \lambda_L^2$ and using the parameters of Table I:

$$\hbar \omega_z = \hbar \sqrt{\frac{\Gamma}{\chi_\pi}} B = \frac{\sqrt{2} \hbar^2}{m^* \lambda_L^2} \simeq 5.9 \mu\text{eV}. \quad (44)$$

We can thus conclude that the presence of the external magnetic field in fact does break the degeneracy of the two gapless Goldstone modes, leaving only one mode gapless while rendering the other massive. The rather small value of the gap, $5.9 \mu\text{eV} \approx 68 \text{ mK}$, would be very difficult to observe in a neutron scattering experiment. It is two orders of magnitude smaller than the π resonance, and hence it is seen to be a good approximation to disregard the interaction between the external magnetic field and the antiferromagnetic order parameter.

B. Inter-layer coupling

To this point we have only treated one single CuO plane. Naturally, to stabilize the order parameter, interaction between the layers has tacitly been assumed. In this section we are explicitly going to include that part of the inter-layer coupling which arises from the antiferromagnetic coupling between the CuO planes. We model this coupling by a Hamiltonian \hat{H}' , where spins at site j in the CuO plane ζ are interacting with the closest spins in the neighboring planes $\zeta \pm 1$ as follows:

$$\hat{H}' = \frac{1}{2}J' \sum_{j,\zeta} \hat{\mathbf{S}}_{j,\zeta} \cdot [\hat{\mathbf{S}}_{j,\zeta-1} + \hat{\mathbf{S}}_{j,\zeta+1}]. \quad (45)$$

The inter-layer coupling J' is much smaller than the intralayer coupling J , namely $J' \simeq 4 \times 10^{-5} J$.²⁵ In this specific model there is no coupling between sites having different in-plane index j , and we are led to consider 1D spin chains perpendicular to the planes. As before, see Eqs. (33) and (34), the spins are represented by the classical fields \mathbf{h} , \mathbf{m} , and \mathbf{l} :

$$\hat{\mathbf{S}}_{j,\zeta} \longrightarrow s(-1)^\zeta \mathbf{h}_{j,\zeta}, \quad \mathbf{h}_{j,\zeta} = \mathbf{m}_{j,\zeta} + (-1)^\zeta \mathbf{l}_{j,\zeta}. \quad (46)$$

Henceforth, we drop the site index j and focus on just one of the spin chains. The Hamiltonian H' is now expressed in terms of the classical fields, and in the continuum limit we obtain the form

$$\hat{H}' \longrightarrow -\frac{J'}{8a^2} \int d^2\mathbf{r} \sum_{\zeta} \{2 - [\mathbf{h}_{\zeta}(\mathbf{r}) - \mathbf{h}_{\zeta-1}(\mathbf{r})]^2\}. \quad (47)$$

Defining $\Delta\mathbf{m}_{\zeta} = \mathbf{m}_{\zeta} - \mathbf{m}_{\zeta-1}$ we obtain the following form of the Lagrange density, \mathcal{L}_{ilc} for the inter-layer coupling:

$$\mathcal{L}_{\text{ilc}} = -\frac{J'}{8a^2} \sum_{\zeta} [2 - \Delta\mathbf{m}_{\zeta}^2]. \quad (48)$$

As in Sec. IV A, excitations $\delta\mathbf{m}$ in the order parameter $\mathbf{m} = m\mathbf{e}_y$ are sought in the perpendicular directions \mathbf{e}_x and \mathbf{e}_z . The motion in these two directions is independent of each another, and we write the excitations $\delta\mathbf{m}_{\beta}$, $\beta = x$ or z , as

$$\delta\mathbf{m}_{\beta}(\zeta) = \theta_{\beta}(\zeta) \mathbf{e}_{\beta}, \quad (49)$$

where the amplitude $\theta_{\beta}(\zeta)$ is m times the (small) angle by which the order parameter m in plane ζ is tilted away from its equilibrium position. The eigenmodes are found by the Fourier transformation

$$\theta_{\beta}(\zeta) = \sum_k \theta_{k,\beta} e^{ik\zeta c}, \quad k = n \frac{2\pi}{N_c c}, \quad n = 1, 2, 3, \dots, \quad (50)$$

where N_c is the number of CuO planes in the sample. Because of the Fourier transform it is more natural to work with Lagrange functions, $L = \int \mathcal{L} d^2\mathbf{r}$, rather than Lagrange densities. However, in the end by dividing L with $N_c \xi^2$, the number of planes times the effective area of a vortex, the Lagrange function is rendered into a Lagrange density. The resulting Lagrangian density $\mathcal{L}_{\text{ilc}}^{(2)}(\delta\mathbf{m}_{\beta})$ thus becomes

$$\begin{aligned} \mathcal{L}_{\text{ilc}}^{(2)}(\delta\mathbf{m}_{\beta}) &= \sum_{k,\beta} \left\{ \frac{\chi}{2} |\partial_t \theta_{k,\beta}|^2 - \frac{J'}{4a^2} [1 - \cos(kc)] |\theta_{k,\beta}|^2 \right\} \\ &= \frac{1}{2} \chi \sum_{k,\beta} [|\partial_t \theta_{k,\beta}|^2 - \omega_{k,\beta}^2 |\theta_{k,\beta}|^2], \quad (51) \end{aligned}$$

where, after using $\chi = \hbar^2/8Ja^2$, the eigenfrequencies $\omega_{k,\beta}$ are seen to be

$$\hbar\omega_{k,\beta} = 2\sqrt{J'J[1 - \cos(kc)]}. \quad (52)$$

The inter-layer coupling thus splits the $2N_c$ -fold degenerate Goldstone modes in a stack of N_c vortices. The two $k = 0$ modes, $\omega_{0,\beta} = 0$, remain zero energy modes. However, since $\omega_{k,(x,z)} = \omega_{2\pi-k,(x,z)}$, the rest of the modes, $k > 0$, split up in a quasi continuous band consisting of $N_c/2 - 1$ four-fold degenerate massive Goldstone modes. The most massive modes are found for $k = \pi/c$ with an energy

$$\hbar\omega_{\pi/c,\beta} = \sqrt{8J'J} \simeq 2.2 \text{ meV} \approx 26 \text{ K}. \quad (53)$$

We note that for two-layer compounds such as YBCO the effect of the inter-layer coupling can be estimated by setting $N_c = 2$ in the above calculation. In this case only $k = 0$ and $k = \pi/c$ occurs, and the degeneracy splitting is given by the stated 2.2 meV or 26 K. We conclude that also the inter-layer coupling produces only minor effects in the excitation spectrum as compared to the π excitation, however, the estimated splitting of 2.2 meV is resolvable with the existing neutron scattering spectrometers. For completeness we note that the combined effect of the external magnetic field and the inter-layer coupling on the Goldstone modes is given by $\omega = \sqrt{\omega_{\beta}^2 + \omega_{k,\beta}^2}$.

V. CONCLUSIONS

The excitations in the antiferromagnetic cores of superconducting vortices in the $SO(5)$ model have been studied. By examining the existing literature on experimental results connecting to the values of the parameters of the model, we have found that the stiffnesses in the charge and spin sectors are nearly identical, $\rho_c \approx \rho_s$, and likewise for the susceptibilities, $\chi_c \approx \chi_s$. This remarkable fact serves as good support of the idea of the existence of a $SO(5)$ symmetry in the high T_c cuprates.

We have predicted within the $SO(5)$ model that bound localized excitations exist when asymmetries arise between the π sector of the parameters and the spin and charge sectors. If they exist, these excitations could be observed in neutron scattering experiments as side peaks to the already observed π excitation, side peaks with an amplitude proportional to the number of vortices and thereby proportional to the applied external magnetic field.

Finally, we have predicted the splitting of the degenerate zero energy mode as a function of applied magnetic field and the inter-layer coupling. The effect of the magnetic field is minute, only a few μeV , and thus not possible to detect with present day neutron scattering technology. The effect of the inter-layer coupling, on the other hand, is of the order of 2 meV and hence detectable in inelastic neutron scattering experiments. The test of

the existence of these core excitations would constitute a crucial test of the $SO(5)$ model. The expected signal should only be present in the superconducting phase, and it should be proportional with the number of vortices, *i.e.* with the applied magnetic field.

VI. ACKNOWLEDGEMENTS

We thank Niels Hessel Andersen and Poul Erik Lindelof for useful discussions concerning the experimental possibilities. H.B. is supported by the Danish Natural Science Research Council through Ole Rømer Grant No. 9600548.

- ²³ J. Gan and P. Hedegård Phys. Rev. B **53**, 911 (1996).
²⁴ E. Fradkin, *Field Theories of Condensed Matter Systems*, Frontiers in Physics Vol. 82 (Addison-Wesley Publishing Company, New York, 1991).
²⁵ S-W. Cheong, Thompson, and Z. Fisk, Phys. Rev. B **39**, 4395 (1989).

-
- ¹ H. A. Mook, M. Yethiraj, G. Aeppli, T. E. Mason, and T. Armstrong Phys. Rev. Lett. **70**, 3490 (1993).
² H. F. Fong, B. Keimer, P. W. Anderson, D. Reznik, F. Dogan, and I. A. Aksay Phys. Rev. Lett. **75**, 316 (1995).
³ P.W. Anderson, Science, **235**, 1196 (1987).
⁴ F.C. Zhang and T.M. Rice, Phys. Rev. B **37**, 3759 (1988).
⁵ E. Demler and S.-C. Zhang, Phys. Rev. Lett. **75**, 4126 (1995).
⁶ S.-C. Zhang, Science, **275**, 1089 (1997).
⁷ G. Baskaran and P.W. Anderson, Report No. cond-mat/9706076.
⁸ M. Greiter, Phys. Rev. Lett. **79**, 4898 (1997), and Report No. cond-mat/9705282.
⁹ E. Demler, S.-C. Zhang, S. Meixner, and W. Hanke Phys. Rev. Lett. **79**, 4937 (1997)
¹⁰ R.B. Laughlin, Report No. cond-mat/9709197.
¹¹ D. Arovas, A. J. Berlinsky, C. Kallin and S.-C. Zhang, Phys. Rev. Lett. **79**, 2871 (1997).
¹² N. H. Andersen, unpublished work at Risø National Laboratory (1998).
¹³ E. Dagotto, Rev. Mod. Phys. **66**, 763 (1994), and references therein.
¹⁴ D. N. Zheng, A. M. Cambell, J. D. Johnson, J. R. Cooper, F. J. Blunt, A. Porch, and P. A. Freeman, Phys. Rev. B **49**, 1417 (1994).
¹⁵ B. Pümpin, H. Keller, W. Kündig, W. Odermatt, I.M. Savić, J.W. Schneider, H. Simmler, P. Zimmermann, E. Kaldis, S. Rusiecki, Y. Maeno, and C. Rossel, Phys. Rev. B **42**, 8019 (1990).
¹⁶ S. Chakravarty, B. I. Halperin, and D. R. Nelson, Phys. Rev. B **39**, 2344 (1989).
¹⁷ E. Manousakis, Rev. Mod. Phys. **63**, 1 (1991),
¹⁸ J. Igarashi, Phys. Rev. B **46**, 10 763 (1992).
¹⁹ S.M. Hayden, G. Aeppli, A.D. Taylor, T.G. Perring, S-W. Cheong, and Z. Fisk, Phys. Rev. Lett. **67**, 3622 (1991).
²⁰ B. Keimer *et al.*, Phys. Rev. B **46**, 14 034 (1992).
²¹ S.M. Hayden, G. Aeppli, T.G. Perring, H. A. Mook, and F. Dogan, Phys. Rev. B **54**, R6905 (1996).
²² P. W. Anderson, Phys. Rev. **130**, 439 (1963).